NASA/TM—2006-214336

Solar Effects on Tensile and Optical Properties of Hubble Space Telescope Silver-Teflon® Insulation

Kim K. de Groh, Joyce A. Dever, and Aaron Snyder
Glenn Research Center, Cleveland, Ohio

Sharon Kaminski, Catherine E. McCarthy, Allison L. Rapoport, and Rochelle N. Rucker
Hathaway Brown School, Shaker Heights, Ohio

October 2006

NASA STI Program . . . in Profile

Since its founding, NASA has been dedicated to the advancement of aeronautics and space science. The NASA Scientific and Technical Information (STI) program plays a key part in helping NASA maintain this important role.

The NASA STI Program operates under the auspices of the Agency Chief Information Officer. It collects, organizes, provides for archiving, and disseminates NASA's STI. The NASA STI program provides access to the NASA Aeronautics and Space Database and its public interface, the NASA Technical Reports Server, thus providing one of the largest collections of aeronautical and space science STI in the world. Results are published in both non-NASA channels and by NASA in the NASA STI Report Series, which includes the following report types:

- TECHNICAL PUBLICATION. Reports of completed research or a major significant phase of research that present the results of NASA programs and include extensive data or theoretical analysis. Includes compilations of significant scientific and technical data and information deemed to be of continuing reference value. NASA counterpart of peer-reviewed formal professional papers but has less stringent limitations on manuscript length and extent of graphic presentations.

- TECHNICAL MEMORANDUM. Scientific and technical findings that are preliminary or of specialized interest, e.g., quick release reports, working papers, and bibliographies that contain minimal annotation. Does not contain extensive analysis.

- CONTRACTOR REPORT. Scientific and technical findings by NASA-sponsored contractors and grantees.

- CONFERENCE PUBLICATION. Collected papers from scientific and technical conferences, symposia, seminars, or other meetings sponsored or cosponsored by NASA.

- SPECIAL PUBLICATION. Scientific, technical, or historical information from NASA programs, projects, and missions, often concerned with subjects having substantial public interest.

- TECHNICAL TRANSLATION. English-language translations of foreign scientific and technical material pertinent to NASA's mission.

Specialized services also include creating custom thesauri, building customized databases, organizing and publishing research results.

For more information about the NASA STI program, see the following:

- Access the NASA STI program home page at *http://www.sti.nasa.gov*

- E-mail your question via the Internet to *help@sti.nasa.gov*

- Fax your question to the NASA STI Help Desk at 301–621–0134

- Telephone the NASA STI Help Desk at 301–621–0390

- Write to:
  NASA STI Help Desk
  NASA Center for AeroSpace Information
  7121 Standard Drive
  Hanover, MD 21076–1320

NASA/TM—2006-214336

Solar Effects on Tensile and Optical Properties of Hubble Space Telescope Silver-Teflon® Insulation

Kim K. de Groh, Joyce A. Dever, and Aaron Snyder
Glenn Research Center, Cleveland, Ohio

Sharon Kaminski, Catherine E. McCarthy, Allison L. Rapoport, and Rochelle N. Rucker
Hathaway Brown School, Shaker Heights, Ohio

Prepared for the
2006 Spring Meeting
sponsored by the Materials Research Society
San Francisco, California, April 17–21, 2006

National Aeronautics and
Space Administration

Glenn Research Center
Cleveland, Ohio 44135

October 2006

Acknowledgments

The authors would like to thank the European Space Agency and the Hubble Project Office at Goddard Space Flight Center, and in particular Ben Reed, for providing the HST insulation sample for these analyses. They would like to thank Janet Hodermarsky of Ohio Aerospace Institute for conducting the initial photo-documentation and the tensile tests. The authors also greatly appreciate the thermal modeling support provided by Joshua Abel and Elisabeth Abel of Lockheed Martin at Goddard Space Flight Center. Finally, they would like to thank David Bretz of the Image Science and Analysis Group for helping to provide numerous high-resolution images of the Hubble Space Telescope during various servicing missions.

Level of Review: This material has been technically reviewed by technical management.

Available from

NASA Center for Aerospace Information
7121 Standard Drive
Hanover, MD 21076–1320

National Technical Information Service
5285 Port Royal Road
Springfield, VA 22161

Available electronically at http://gltrs.grc.nasa.gov

Solar Effects on Tensile and Optical Properties of Hubble Space Telescope Silver-Teflon® Insulation

Kim K. de Groh, Joyce A. Dever, and Aaron Snyder
National Aeronautics and Space Administration
Glenn Research Center
Cleveland, Ohio 44135

Sharon Kaminski, Catherine E. McCarthy, Allison L. Rapoport, and Rochelle N. Rucker
Hathaway Brown School
Shaker Heights, Ohio 44122

Abstract

A section of the retrieved Hubble Space Telescope (HST) solar array drive arm (SADA) multilayer insulation (MLI), which experienced 8.25 years of space exposure, was analyzed for environmental durability of the top layer of silver-Teflon (DuPont) fluorinated ethylene propylene (Ag-FEP). Because the SADA MLI had solar and anti-solar facing surfaces and was exposed to the space environment for a long duration, it provided a unique opportunity to study solar effects on the environmental degradation of Ag-FEP, a commonly used spacecraft thermal control material. Data obtained included tensile properties, solar absorptance, surface morphology and chemistry. The solar facing surface was found to be extremely embrittled and contained numerous through-thickness cracks. Tensile testing indicated that the solar facing surface lost 60% of its mechanical strength and 90% of its elasticity while the anti-solar facing surface had ductility similar to pristine FEP. The solar absorptance of both the solar facing surface (0.155 ± 0.032) and the anti-solar facing surface (0.208 ± 0.012) were found to be greater than pristine Ag-FEP (0.074). Solar facing and anti-solar facing surfaces were microscopically textured, and locations of isolated contamination were present on the anti-solar surface resulting in increased localized texturing. Yet, the overall texture was significantly more pronounced on the solar facing surface indicating a synergistic effect of combined solar exposure and increased heating with atomic oxygen erosion. The results indicate a very strong dependence of degradation, particularly embrittlement, upon solar exposure with orbital thermal cycling having a significant effect.

Introduction

The Hubble Space Telescope was launched on April 25, 1990 into low Earth orbit as the first mission of NASA's Great Observatories program. The HST was designed to be serviced on-orbit to upgrade scientific capabilities. In December 1993, during the first servicing mission (SM1) the original solar arrays (SA-I) were replaced with a second set of arrays (SA-II) containing bi-stem thermal shields to eliminate a thermal induced jitter problem. In March of 2002, after 8.25 years of space exposure, the SA-II was replaced with a third set of arrays (SA-III) during the fourth servicing mission (SM3B), and the SA-II was brought back to Earth. A section of the retrieved SA-II solar array drive arm (SADA) multilayer insulation (MLI) was provided to NASA Glenn Research Center so that environmental durability analyses of the top layer of silver-Teflon (DuPont) fluorinated ethylene propylene (Ag-FEP) could be conducted.

The SADA MLI was wrapped completely around the SADA and therefore had solar and anti-solar facing surfaces (see fig. 1). The circular configuration of the insulation, along with the long-term space exposure, provided a unique opportunity to study solar radiation effects on the environmental degradation of Ag-FEP, a commonly used spacecraft thermal control material. The objective of this research was to characterize the degradation of retrieved HST SADA Ag-FEP after 8.25 years of space exposure with

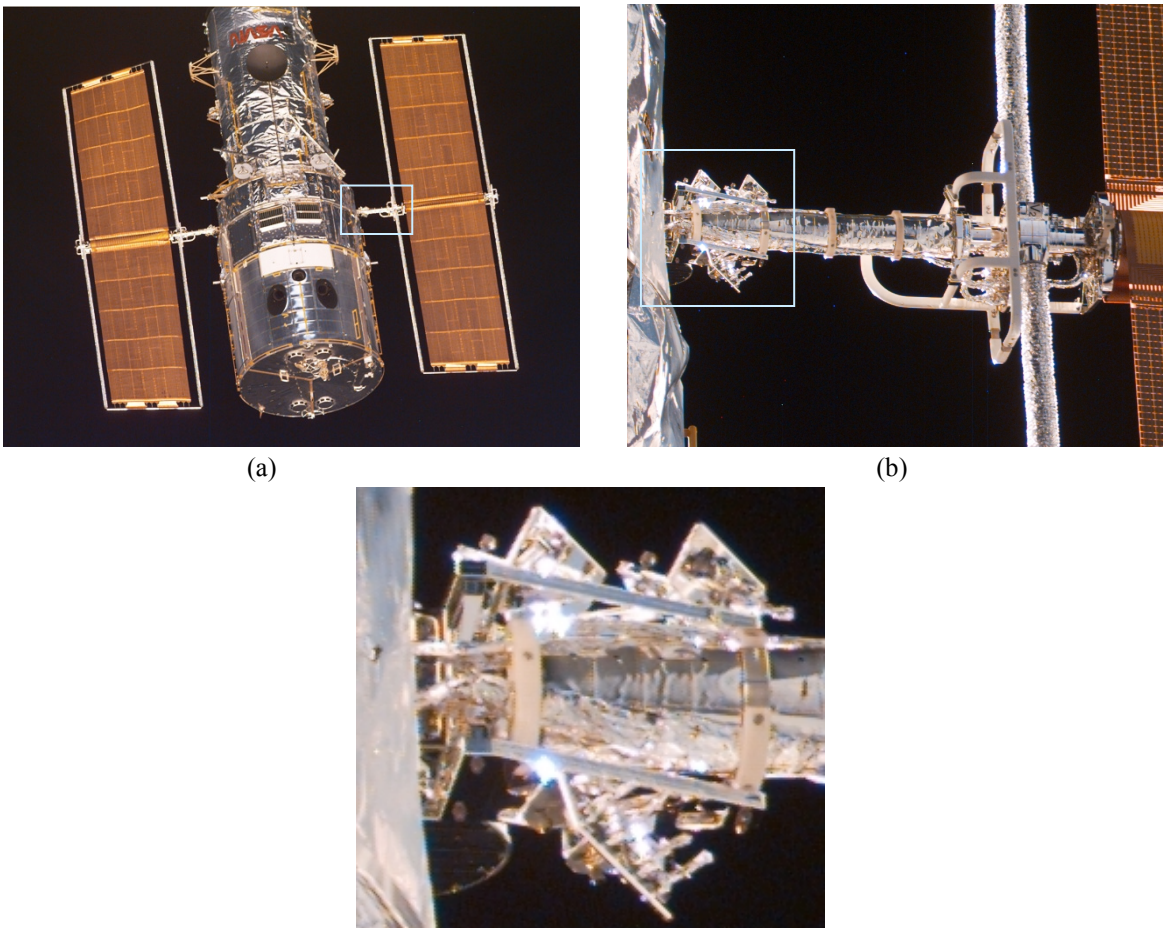

(a) (b)

(c)

Figure 1. Hubble Space Telescope photographed in December 1999 during the third servicing mission (SM3A), viewed from the –V3 side: (a) HST with SA-II, indicating the +V2 SADA, (b) Close-up of the +V2 MLI covered SADA and (c) Close-up of the in-board SADA section.

particular emphasis on the effect of solar exposure. Data obtained included tensile properties, solar absorptance, surface morphology and chemistry.

Materials and Environmental Exposure

HST SM3B SA-II SADA MLI

The retrieved SA-II SADA MLI sample used in this study was provided by the European Space Agency (ESA) and is shown in figure 2. The sample was 36.9 by 9.1 cm. The sample's top layer is approximately 10 mil (0.25 mm) thick, consisting of a space-exposed 5 mil (127 μm) Teflon FEP layer coated on the backside with vapor deposited silver and Inconel (the Ag layer is 1500 Å thick and the Inconel layer is 275 Å thick). The FEP/Ag/Inconel layer is adhered with an acrylic adhesive (40 μm thick 966 acrylic) to a fiberglass cloth impregnated with polytetrafluoroethylene (PTFE). The MLI has 16 layers of double-sided aluminized-Kapton (DuPont) (50 μm thick) separated by Dacron (DuPont) netting and a bottom layer of PTFE-impregnated fiberglass cloth. All analyses were obtained from the top layer of insulation (FEP/Ag/ Inconel/adhesive/ scrim), referred to in this report as Ag-FEP.

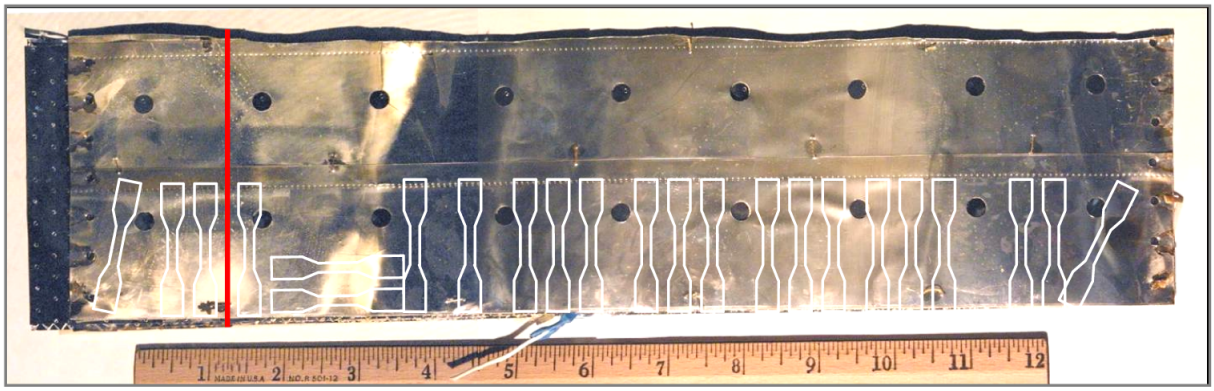

Figure 2. The HST SADA MLI sample (the line indicates the solar facing position (0°)).

This sample was cut from the +V2 SADA MLI section closest to the body of the telescope, or the in-board section (see figs. 1(b) and (c)). The V2 axis passes through the SADAs and the +V2 solar array is shown on the right in figure 1(a). For this study, 0° has been defined as the direct solar-facing surface (indicated as a line in fig. 2) and 180° is the anti-solar facing surface, with 90° and 270° being solar grazing surfaces. The exact position on the MLI sample that was directly solar facing was not known. Therefore, the 0° position was chosen based on the center of the discolored solar-facing region (described below). Pristine 5 mil (127 μm) thick Ag-FEP (without the adhesive or scrim) was used for obtaining pristine solar absorptance data and five pristine 5 mil (127 μm) thick FEP (non-metallized) samples were used for obtaining pristine tensile properties.

Environmental Exposure

The estimated environmental exposure conditions for the SA-II SADA Ag-FEP, installed during SM1 and retrieved during SM3B, are given in table 1, showing comparison to exposure conditions from the time of HST's deployment in April 1990 to each HST servicing mission and estimations of conditions through December 2010. Data from references 1 to 3 were used as the basis for estimating the environment exposure conditions. Environmental exposure conditions for the HST SA-I retrieved during SM1 were described in references 1 and 2. Environmental exposure conditions for SM1 through December 2010 were described in reference 3. It should be noted that cabling and other components covered areas of the SADA MLI insulation, primarily on solar grazing surfaces, as shown in figures 1(b) and 1(c). Also, Bay J, one of several small bays positioned on the anti-solar side of the telescope, is covered with aluminized-FEP MLI and could provide scattered atomic oxygen arrival to the anti-solar in-board SADA in addition to sweeping atomic oxygen arrival. Figure 3 shows a close-up photograph taken during SM3A from the anti-solar side of the telescope showing Bay J and the +V2 SADA. The in-board SADA might also receive somewhat reduced electron, proton and albedo UV radiation exposure on the anti-solar side compared to the solar side, due to the presence of Bay J (no bay is present on the solar side).

The HST mission timeline was used to determine the number of orbits and, therefore, the number of thermal cycles experienced from deployment to SM2.[3] In order to calculate the number of thermal cycles for SM3A, SM3B and December 2010, it is assumed that the average HST orbital period is 96 minutes. The equivalent solar exposure hours (ESH) data in table 1 assume that the average HST orbit provides 32% of time in shadow, based on the variation of time-in-shadow between approximately 27 and 37%.[3] The SA-I environmental conditions reported in reference 2 assumed 38% time in shadow. Based on the 27 to 38% reported variation in percent of orbital shadow, error on calculated ESH is estimated

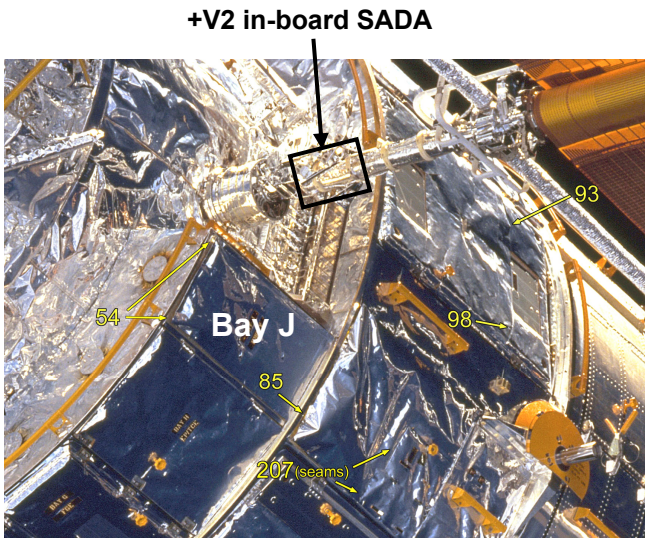

Figure 3. Close-up photograph of HST taken during SM3A from the anti-solar side of the telescope showing Bay J and the +V2 SADA.

to be ±11%. Equivalent Earth albedo solar exposure hours are also shown in table 1. These data assume that directly solar-facing SADA surfaces receive Earth albedo illumination equivalent to 2.3% of direct solar exposure, and Earth albedo incident on anti-solar surfaces is equivalent to approximately 32% of direct solar exposure.[2]

Data for x-ray fluence in table 1 were based on x-ray flux data from the Geosynchronous Operational Environmental Satellites (GOES) for the time period of launch (1990) through SM2 (February 1997).[3] For SM2 through 2010, the x-ray fluence was estimated assuming an average 11-year solar cycle.[3] Because x-ray exposure is primarily due to solar events, it is assumed that only solar facing surfaces receive x-rays and that anti-solar surfaces receive no x-ray exposure. HST was launched during a time of solar maximum; therefore, x-ray flux was high in the early part of the mission and decreased as solar minimum was reached around 1997. The next solar maximum peak is assumed to have been around 2001. Electron and proton fluence from solar wind particles trapped in Earth's magnetic field have been calculated previously using NASA's proton and electron models, AP-8 and AE-8, respectively.[3] The data for SM3B were extrapolated from these prior data. Electron and proton fluence is assumed to be omni-directional, providing exposure to both solar and anti-solar facing surfaces.

Atomic oxygen ram fluence values for HST indicated in table 1 were modeled based on the Mass Spectrometer Incoherent Scatter Model 86 (MSIS-86).[3] Using the ram fluence values for each HST servicing mission, atomic oxygen fluences for solar-facing and anti-solar facing surfaces were obtained using equations (1) and (2), respectively.[3]

$$Fluence_{\,solar\text{-}facing} \approx Fluence_{\,ram} \times 0.2528 \times 0.5 \tag{1}$$

$$Fluence_{\,anti\text{-}solar} \approx Fluence_{\,ram} \times 0.3167 \times 0.5 \tag{2}$$

The solar-facing and anti-solar atomic oxygen fluence values are provided in table 1. Equations (1) and (2) use flux ratios for solar-facing/ram and anti-solar/ram determined for International Space Station surfaces.[4] Equations (1) and (2) also assume that the SADA is close enough to the body of HST to have a view of only one half the angles seen by unobstructed surfaces, resulting in half of the fluence that would be incident on unobstructed surfaces (hence the 0.5 factor).

Table 1. Environmental Exposure Conditions for HST Ag-FEP Surfaces

Exposure		Deploy to SM1 (SA-I)	Deploy to SM2	Deploy to SM3A	Deploy to SM3B	SM1 to SM3B (SA-II)	Deploy to Dec. 2010
Missions		STS-31 STS-61	STS-31 STS-82	STS-31 STS-103	STS-31 STS-109	**STS-61** **STS-109**	STS-31 N/A
Mission dates		April 1990 Dec. 1993	April 1990 Feb. 1997	April 1990 Dec. 1999	April 1990 March 2002	**Dec. 1993** **March 2002**	April 1990 N/A
Exposure (yr)		3.6	6.8	9.7	11.9	**8.25**	20.7
Thermal cycles (#)		19,700	37,100	52,800	64,800	**45,100**	~110,000
Temperature range (°C)		**BOL Solar facing: -82 to -20 & Anti-solar facing: -137 to -30** **EOL Solar facing: -60 to +30 & Anti-solar facing: -118 to + 5** SA I SADA, estimated: -100 to >+100 [1]					
ESH, Solar-facing	Direct	~21,500	~40,600	~57,500	~70,600	**~49,100**	~123,000
	Albedo	~500	~930	~1,300	~1,600	**~1,100**	~2,800
	Total	~22,000	~41,530	~58,800	~72,200	**~50,200**	~126,000
ESH, Anti-solar (albedo only)		6,900	13,000	18,400	22,500	**15,600**	39,300
X-ray fluence (J/m^2)	1-8 Å	222.6	252.4	302.2	382.6	**160.0**	699.6
	0.5-4 Å	14.7	16.0	19.1	24.8	**10.1**	47.2
Electron fluence ($\#/cm^2$) > 40 keV		1.39×10^{13}	1.95×10^{13}	2.74×10^{13}	3.47×10^{13}	**2.08×10^{13}**	6.04×10^{13}
Proton fluence ($\#/cm^2$) > 40 keV		7.96×10^{9}	1.95×10^{10}	2.77×10^{10}	3.35×10^{10}	**2.55×10^{10}**	5.86×10^{10}
Atomic oxygen fluence ($atoms/cm^2$)	Ram	9.6×10^{20}	1.0×10^{21}	[a]1.8×10^{21}	2.2×10^{21}	**1.2×10^{21}**	$3.4\text{-}3.5 \times 10^{21}$
	Solar	1.2×10^{20}	1.3×10^{20}	2.3×10^{20}	2.7×10^{20}	**1.5×10^{20}**	4.4×10^{20}
	Anti-solar	1.5×10^{20}	1.6×10^{20}	2.8×10^{20}	3.4×10^{20}	**1.9×10^{20}**	5.5×10^{20}

[a]In reference 3, atomic oxygen fluence was calculated assuming a mission date of June 2000. The fluence shown in table 1 has been linearly interpolated for the actual mission date (December 1999).

Temperature range estimates for the solar facing and anti-solar facing SA-II drive arm MLI were provided by Goddard Space Flight Center.[5] These values were computed using the HST Detailed SA-III Thermal Model using a representative geometric shape for SA-II. Four cases were run to get temperature extremes:

1) ***Cold attitude for the sun side****: beginning-of-life (BOL) optical properties, cold environmental fluxes (this provides the minimum temperature on the sun side)*
2) ***Hot attitude for the sun side****: end-of-life (EOL) optical properties, hot environmental fluxes (this provides the maximum temperature on the sun side)*
3) ***Cold attitude for shade side****: BOL optical properties, cold environmental fluxes (this provides the minimum temperature on the shade side)*
4) ***Hot attitude for shade side****: EOL optical properties, hot environmental fluxes (this provides the maximum temperature on the shade side)*

Beginning-of-life solar absorptance (α_s) and thermal emittance (ε) of 0.08 and 0.81, respectively were used. End-of-life α_s and ε values of 0.187 (0.155 ± 0.032) and 0.81, respectively, were used (see Solar Absorptance results section). For the hot attitude case the solar flux was 1,419 W/m^2, the albedo was 0.35 and the Earth's infrared (IR) was 265 W/m^2. For the cold attitude case the solar flux was

1,286 W/m^2, the albedo was 0.25 and the Earth's IR was 208 W/m^2. There was no conduction considered between blanket nodes (i.e., the surface of the blanket). However, a blanket emittance to the mast of 0.03 was included, along with conduction in the mast in both the radial and lateral directions. Using the listed BOL and EOL optical properties, the resulting temperature estimates are lower than those provided by European Space Agency (-100 to +100 °C) in reference 1.

Experimental Procedures

Optical and Electron Microscopy

An Olympus SZH microscope operated with a Canon EOS D30 digital camera was used to document various features of the sample at magnifications on the order of 10X to 100X. Scanning electron microscope images were obtained using a Hitachi S-4700 field emission scanning electron microscope (FESEM) operated at an accelerating voltage of 6 kV. Energy dispersive spectroscopy (EDS) was conducted using an EDAX CDU Leap Detector system.

Tensile Properties

Tensile properties (ultimate tensile strength (UTS) and elongation at failure) were obtained using a DDL Inc. Model 200Q Electromechanical Test System. Twenty-three samples were punched out of the MLI sample (see fig. 2) using a die fabricated to the specifications defined in the American Society for Testing and Materials (ASTM) Standard D-638 for Type V tensile specimens.[6] The "dog-bone" tensile samples had a length of 63.4 mm and width of 9.52 mm, with a 7.62 mm long and 3.18 mm wide neck region. Care was taken to avoid cracks and impact sites and hence tensile samples were not obtained at precise angular intervals. The initial grip separation distance was set for 25.4 mm and testing was conducted at a speed of 1.072 mm/sec. Stress versus strain graphs were produced for each of the tested samples. For computation of UTS the thickness was set to 0.010 in. (0.254 mm) to take into account the total thickness of the sample (FEP/Ag/Inconel/adhesive/scrim), even though the FEP thickness is only 0.005 in. (0.127 mm). Thus, the UTS values for the HST SADA Ag-FEP are not comparable with pristine FEP, which does not have the added adhesive and scrim layer.

The HST SADA Ag-FEP stress versus strain graphs had three distinct steps indicating breakage of three distinct layers. The scrim layer broke with very little elongation, followed by breakage of the FEP layer, and finally breakage of the ductile adhesive layer. Therefore, the UTS and elongation at failure of the FEP layer was determined based on the location of the second step (break of the FEP) on the stress versus strain graphs. See figure 4 for an example.

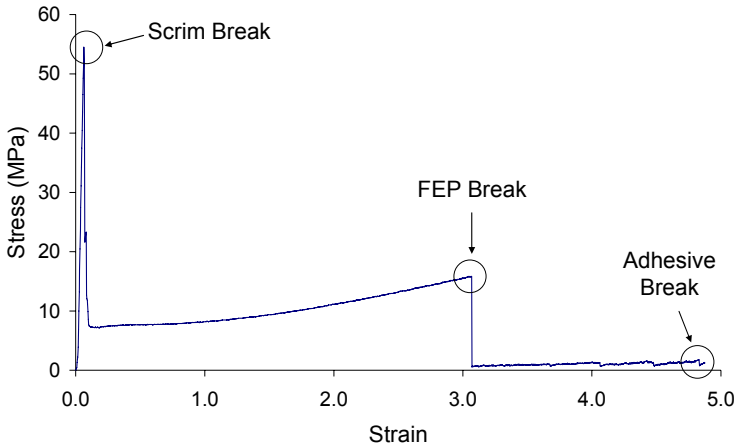

Figure 4. Stress-strain curve for Tensile Sample 5 (295.6°) showing three break points.

Solar Absorptance

An AZ Technology Laboratory Portable SpectroReflectometer 200 (LPSR-200) was used to measure total hemispherical spectral reflectance in the 250 to 2500 nm wavelength range. The LPSR-200 automatically integrates the reflectance data to calculate solar absorptance in accordance with standard methods described in reference 7. Since the sample was embrittled, care was taken to keep the sample flat during data acquisition. Data were originally taken at 9 different solar angle locations. Solar absorptance data were then taken at an additional 52 positions along the top section of the sample (the section above the dog bone samples shown in fig. 2). Three readings were taken at each of the 52 locations and averaged. It should be noted that the position of the absorptance values (with respect to solar angle) may have some error as the sample was not sectioned, but was positioned underneath the LPSR-200. Hence, exact locations were more difficult to determine than for the tensile samples.

Thermal emittance (ε) typically does not change due to environmental exposure unless substantial erosion has occurred. Hence an emittance of 0.81, reported in reference 8, was used for both the pristine and HST SADA 5 mil (0.127 μm) thick Ag-FEP.

Results and Discussion

Optical Microscopy

The HST SADA sample had distinct areas with varying discoloration. In general, the solar-facing region had a non-uniform hazy-white, almost milky appearance, and contained numerous through-thickness cracks. Two of these through-thickness cracks are shown in figure 5. Some areas in the solar facing region were discolored brown. There was no observable darkening long the cracks, hence no significant oxidation of the underlying Ag layer was observed. The solar grazing surfaces had clearer appearances, similar to pristine Ag-FEP, and did not contain cracks. The anti-solar facing side was uniformly hazy-white in appearance, but did not contain any observable cracks.

Tensile Properties

Polar plots of UTS and elongation at failure versus solar angle are provided in figure 6. As can be seen, the solar facing surfaces (0°) are severely embrittled as witnessed by significant decreases in both the UTS and elongation. The UTS and elongation at failure of pristine FEP were 27.4 ± 1.2 MPa and 285.3 ± 15.5%, respectively. Although direct comparison of the UTS values cannot be made with pristine FEP because of the thickness differences, large differences in the UTS are observed for the SADA MLI as a function of solar angle, as shown in figure 6(a). The average UTS of the anti-solar facing surface is

Figure 5. Close-up of the solar facing side of the SADA MLI showing through-thickness cracks and discolored regions.

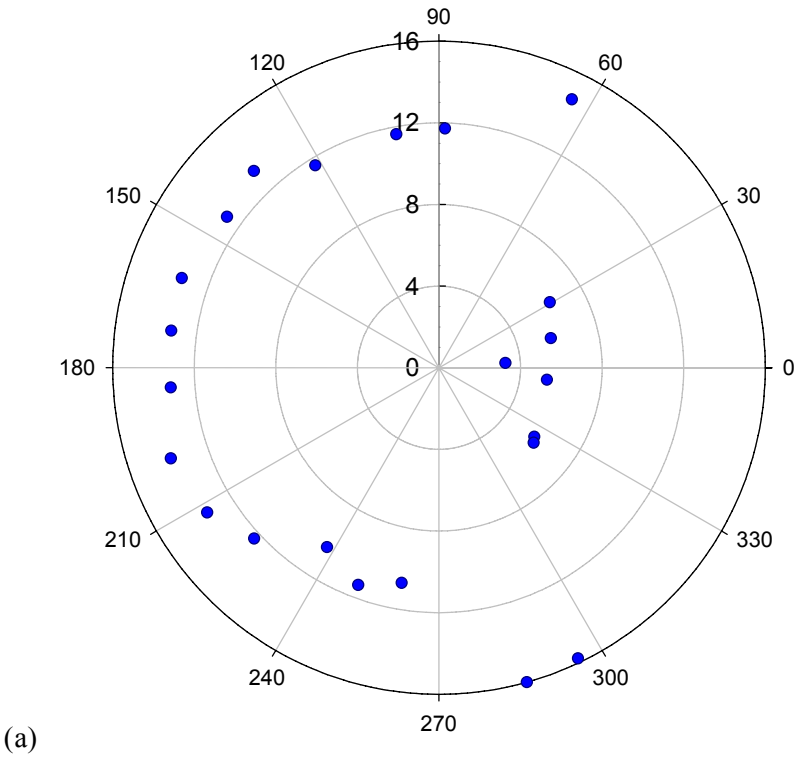

(a)

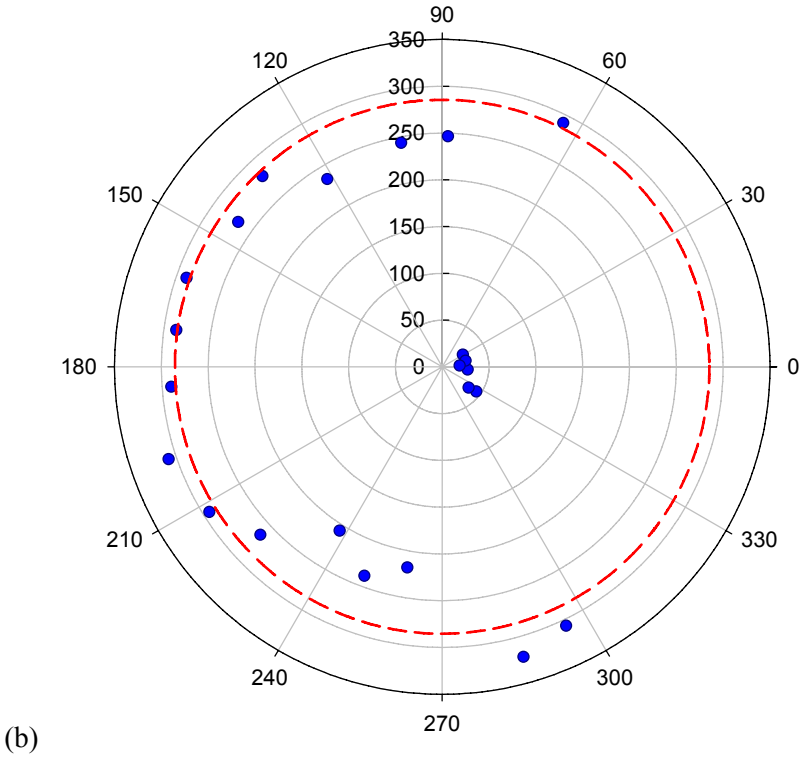

(b)

Figure 6. Polar plots of the HST SADA Ag-FEP tensile data: (a) UTS (MPa) versus solar angle, and (b) Elongation at failure (%) vs. solar angle (the dashed line is for pristine FEP).

13.2 ± 0.5 MPa (average of 8 data points between 133° and 223°). The solar grazing surfaces have very similar average UTS values: 12.4 ± 1.5 MPa for 4 data points between 64° and 122° and 12.4 ± 1.5 MPa for 5 data points between 238° and 296°. These values are slightly lower than the average anti-solar facing UTS. The solar facing surface has greatly decreased average UTS of 5.4 ± 1.1 MPa (averaged from 6 data points between 31° and 322°). This is a 60% decrease compared to the anti-solar surface UTS.

Elongation at failure is not dependent on sample thickness; therefore, the elongation at failure of the HST SADA Ag-FEP can be directly compared with that of pristine FEP, as shown in the polar plot in figure 6(b). By comparing the SADA Ag-FEP elongation to that of pristine FEP (shown as a dashed line), it is apparent that the anti-solar facing surfaces have elongations (284.8 ± 14.3%) essentially the same as pristine FEP (285.3 ± 15.5%), while the solar grazing surfaces have somewhat decreased elongation as compared with pristine FEP (average elongations of 254.0 ± 25.2% and 258.3 ± 52.7% for data centered on 90° and 270°, respectively). The solar facing surface is extremely embrittled with a greatly decreased elongation averaging only 29.8 ± 9.3%. This is a 90% decrease compared to pristine FEP. Severe embrittlement with through thickness cracking of significantly darkened solar facing sections of the MLI had already occurred after 6 years of space exposure, as photo-documented during SM3A.

A HST MLI Failure Review Board (FRB) was assembled after large cracks were observed in the HST light shield MLI during SM2. Studies conducted by the FRB on retrieved HST FEP insulation and ground testing of pristine FEP indicated that thermal cycling with deep-layer damage from electron and proton radiation are necessary to cause FEP embrittlement with the propagation of cracks along stress concentrations, and damage increases with the combined total dose of electrons, protons, ultraviolet and x-ray radiation along with thermal cycling.[9] The SA-II SADA Ag-FEP results appear somewhat inconsistent with the FRB findings: as electron and proton radiation is omni-directional one would expect the anti-solar facing SADA MLI to be somewhat embrittled. However, the results of these analyses indicate otherwise.

Studies conducted by de Groh et al. and de Groh and Martin have shown the impact of temperature on the degradation of irradiated FEP. These studies provide evidence that the dominant mechanism of degradation of FEP in the space environment is irradiation induced chain scission and that heating allows chain mobility resulting in increased crystallization and therefore increased embrittlement.[10,11] A dynamic thermal model, which computes temperature throughout the orbit and includes heat conduction in the circumferential direction, was developed at Glenn Research Center to determine the variation of temperature versus solar angle for the HST SADA Ag-FEP. An example of the temperature variation is provided in figure 7. This plot was computed for an HST orbit station positioned between the Earth and Sun. At this orbit position, direct solar heating occurs (1,400 W/m^2 = one solar unit) on the solar side, and albedo heating and Earth's IR heating on the anti-solar side. However, to take into account reflection from the body of the telescope onto the solar side of the SADA, an arbitrarily chosen direct solar heating of 1.5 solar units (2,100 W/m^2) was used. The albedo heating factor was 0.35 solar units (490 W/m^2) and the IR heating was 0.19 solar units (265 W/m^2), equivalent to an Earth temperature of -12 °C. Internal heating was not considered in this case. Two plots are shown in figure 7: the lower temperature plot (open circle symbol) was computed using pristine optical properties (α_s = 0.08 and ε = 0.81), thus representing the BOL temperature range. The higher temperature plot (solid circle symbol) was computed using optical properties of the solar facing side of the retrieved insulation (α_s = 0.187 and ε = 0.81), thus representing the EOL temperature range. An alpha of 0.187 (0.155 + 0.032) was used from the values provided in the Solar Absorptance section below. These plots show how the temperature varies from the solar facing to anti-solar facing surfaces, and how increased solar absorptance greatly increases the temperature. The temperature variation between the solar and anti-solar facing surfaces, combined with the presence of solar radiation on the solar facing surface, appears to play an important role in the variation in embrittlement versus solar angle of the Ag-FEP.

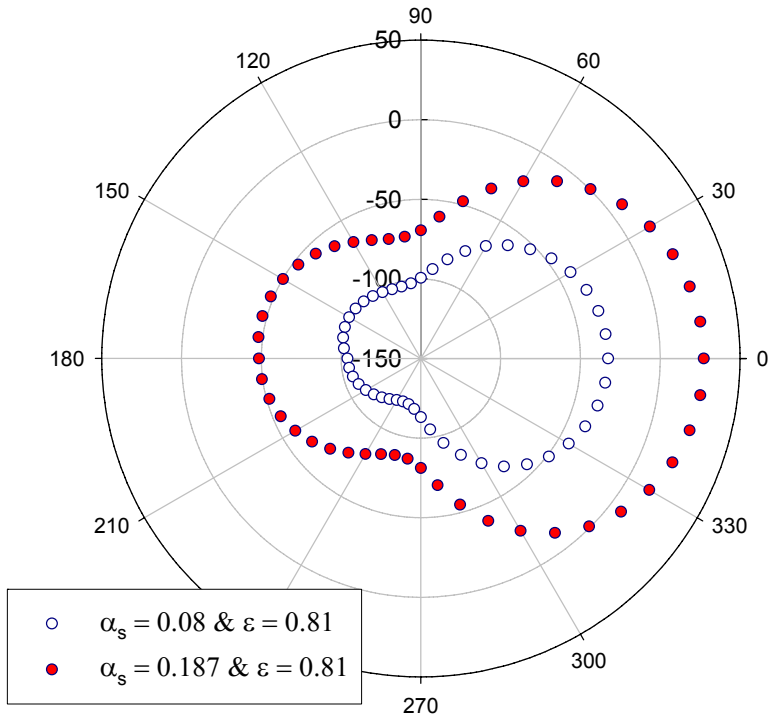

Figure 7. Temperature for the SA-II SADA Ag-FEP as a function of solar angle.

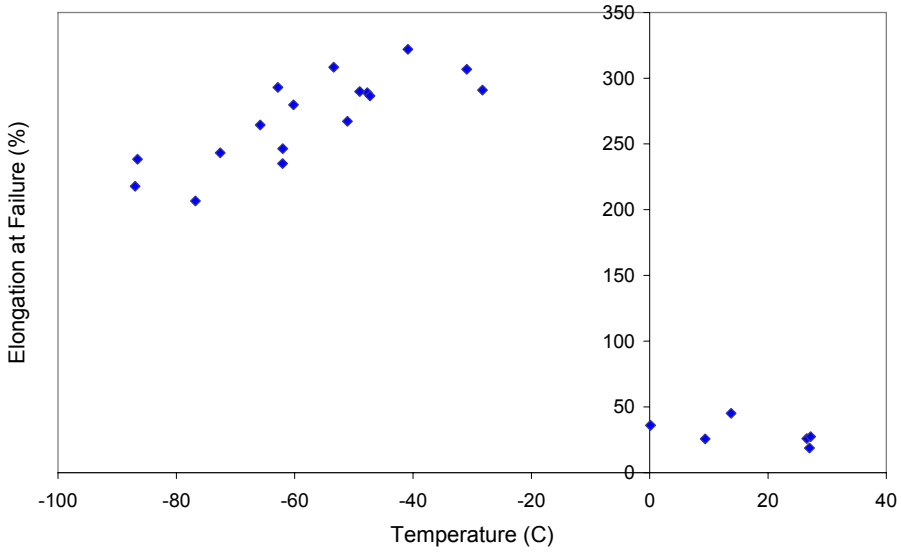

Figure 8. Elongation at failure of the SADA Ag-FEP versus temperature for EOL optical properties based on the Glenn dynamic thermal model.

Using the temperature values computed with the Glenn dynamic thermal model for the EOL optical properties (α_s = 0.187 and ε = 0.81), a graph was made of the elongation at failure versus temperature. This graph is provided in figure 8 and shows a couple different trends. The first is that surfaces heated to the highest temperatures (over 0 °C) were the most dramatically degraded, while the surfaces heated to lower temperatures were still ductile. Yet this plot also shows a trend for decreasing elongation, and

hence embrittlement, for temperatures dropping below -50 °C. Transition temperatures occur in FEP over two broad temperature ranges depending on hexafluoropropylene (HFP) content: between 83 °C and 150 °C.[10] and between -93 and -13 °C.[12] Perhaps the downward trend shown with decreasing temperature in this chart is due to effects of being below the cold transition temperature (during radiation exposure). Although this might be true, the effect is not nearly as deteriorative, with respect to loss of mechanical properties, as the higher temperature exposure.

Solar Absorptance

A polar plot of the solar absorptance versus solar angle is provided in figure 9. The solar absorptance for pristine Ag-FEP was 0.074 and is plotted as a dashed line. As can be seen, the solar absorptance for all 61 locations on the HST SADA MLI is higher than the pristine Ag-FEP solar absorptance. The polar plot shows greater increases in absorptance for the solar and anti-solar surfaces and smaller increases at the solar grazing angles (areas likely shielded by cabling and equipment).

The data was averaged based on 60° angular views centered on 0, 90, 180 and 270°. The solar facing surfaces had an average absorptance of 0.155 ± 0.032 (average of 12 data points between 26.4° and 337.5°) with a large amount of scatter. The scatter in the data corresponds to the variation in haziness and brown discoloration found on the solar facing surfaces. The average solar absorptance values for the two solar grazing surfaces were similar: an average of 0.129 ± 0.027 between 249.6° and 287.9° (average of 10 data points) and 0.134 ± 0.014 between 77° and 114.2° (average of 9 data points). Thus, the overall average for the solar grazing surfaces was 0.131 ± 0.021 (average of 19 data points). Surprisingly, the anti-solar surfaces had high solar absorptance of 0.208 ± 0.012 (average of 11 data points between 151.4° and 201°). The scatter in this data was much smaller than for the solar facing data, which is consistent with the more uniformly hazy appearance of the anti-solar surface.

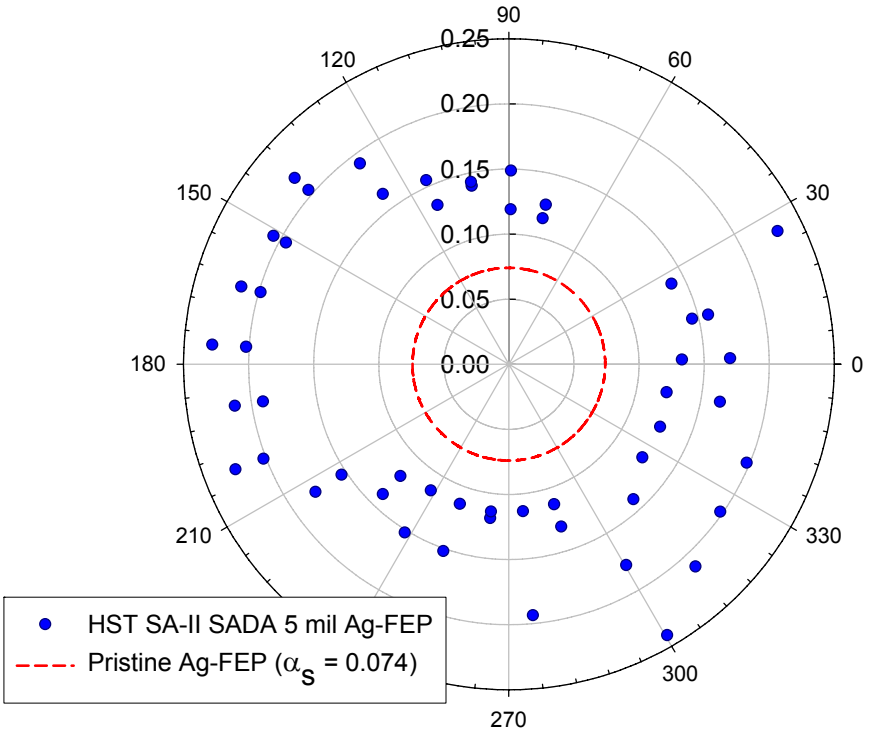

Figure 9. Polar plot of the solar absorptance versus solar angle for the HST SADA Ag-FEP.

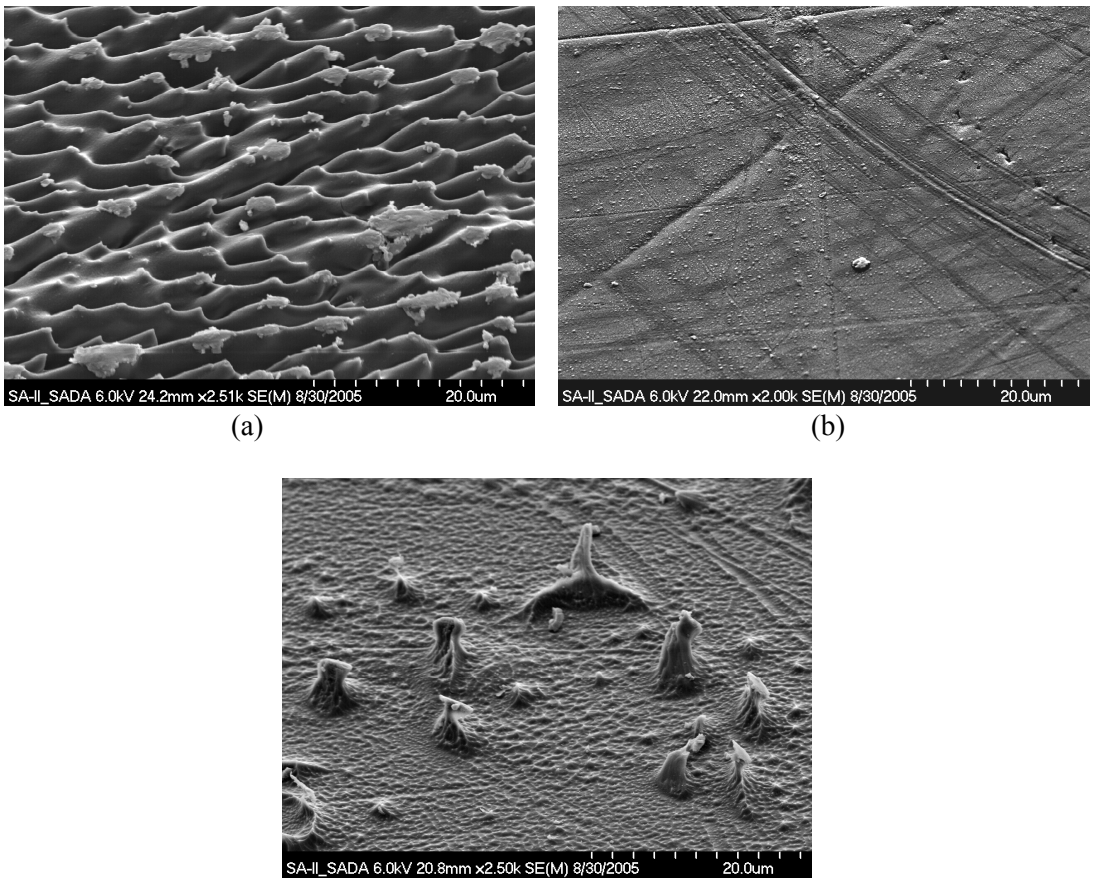

(a) (b)

(c)

Figure 10. Scanning electron microscopy images of SADA Ag-FEP surfaces: (a) Solar facing texture (2.5 kX), (b) Solar grazing texture (2 kX), and (c) Anti-solar facing texture (2.5 kX).

Scanning electron microscopy revealed differences in the texture morphology of the SADA Ag-FEP as a function of solar angle, as shown in figure 10, which appear to correspond to the differences in solar absorptance. The solar facing surface had a wavy rill-like textured morphology, which is attributed to sweeping atomic oxygen erosion (fig. 10(a)). The solar grazing surface was similar to pristine FEP in appearance, smoother with manufacturing lines visible (fig. 10(b)), which is consistent with the location receiving very little atomic oxygen exposure. Yet at very high magnifications, some areas of the solar grazing surfaces are slightly textured as compared to pristine FEP indicating that this particular area was not shielded by cabling or equipment. The anti-solar side was non-uniformly textured (fig. 10(c)). It had an overall texture that was somewhat rougher than the solar grazing surface, but there were non-uniform isolated locations of greater texture where the surface appeared to have been protected from erosion. This surface received slightly higher atomic oxygen exposure than the solar facing surface, so one might expect a similar texture.

Energy dispersive spectroscopy analyses indicated the presence of F, C and O on the "typical texture" areas for all surfaces. Analyses conducted on the tops of the "protected" buttes, such as shown in figure 10, indicate contaminants such as Na and Si, which appear to have provided isolated protection against atomic oxygen erosion.

It has been debated whether there is a synergistic effect of solar exposure on the atomic oxygen erosion of FEP. This study appears to support that theory, as the overall texture is much smoother on the anti-solar side. Perhaps there is a joint effect of simultaneous solar radiation exposure combined with

higher temperature exposure during atomic oxygen exposure resulting in greater texturing on the solar facing surface. One potential complicating factor in this analysis is the contribution of scattered atomic oxygen (and reduced radiation) on this surface from Bay J. Substantial modeling would need to be conducted to determine the extent of atomic oxygen scattering and its possible effect on the erosion depth and texture, which is beyond the scope of this research.

The NASA Glenn Research Center has designed two Materials International Space Station Experiment (MISSE) space exposure experiments, which together will address solar radiation synergistic effects on the atomic oxygen erosion of FEP and other fluoropolymers. One of these experiments has already been flown and retrieved and the other is currently being exposed to the space environment on the exterior of the International Space Station.

Conclusions

A section of retrieved HST SA-II SADA thermal insulation that received 8.25 years of space exposure was provided to NASA Glenn Research Center so that environmental durability analyses of the top layer of Ag-FEP could be conducted. The solar facing surface of the insulation was found to be non-uniformly hazy in appearance and embrittled with numerous through-thickness cracks. Tensile testing indicated that the solar facing surface lost 60% of its mechanical strength and 90% of its elasticity. The anti-solar facing surface was also found to be hazy in appearance, but tensile testing indicated that the anti-solar facing surface had ductility similar to pristine FEP, which was unexpected. Asymmetry of the telescope near the in-board section of the SADA may have resulted in reduced electron, proton and albedo UV radiation of the anti-solar surface. A thermal model was developed to determine temperature versus solar angle for the insulation. Plotting elongation at failure versus temperature indicated a trend of increasing embrittlement for decreasing temperatures below -50 °C, appearing to correspond to a cold transition temperature, but this effect was not nearly as deteriorative as the solar facing higher temperature exposures. These results indicate a very strong dependence of embrittlement on solar exposure, and the effect of temperature appears to play an important role.

The solar absorptance values of the solar facing surface (0.155 ± 0.032) and the anti-solar facing surface (0.208 ± 0.012) were found to have significantly increased compared to the solar absorptance of pristine Ag-FEP (0.074). Scanning electron microscopy and corresponding EDS indicated that both the solar facing and anti-solar facing surfaces were microscopically textured, affecting the solar absorptance, and the anti-solar side had locations of isolated Si contamination that contributed to increased localized texturing. Yet, the overall texture was significantly more pronounced on the solar facing surface, even though it received less atomic oxygen, indicating a synergistic effect of combined solar exposure and increased heating with atomic oxygen erosion. But it should be kept in mind that the anti-solar surface may have received scattered atomic oxygen from Bay J in addition to sweeping atomic oxygen, which would modify the erosion texture. These results provide valuable information on space environmental degradation of Ag-FEP, particularly with respect to solar radiation and temperature effects on embrittlement.

References

[1]M. Van Eesbeek, F. Levadou, and A. Milintchouk, "Investigation on FEP from PDM and Harness from HST-SA1," Proceedings of the Hubble Space Telescope Solar-Array Workshop, Noordwijk, the Netherlands, May 30-31, 1995, ESA WPP-77, 403-416 (1995).

[2]G. Drolshagen, "Definition of the Space Environment for the HST Solar-Array 1," Proceedings of the Hubble Space Telescope Solar-Array Workshop, Noordwijk, the Netherlands, May 30-31, 1995, ESA WPP-77, 53-65 (1995).

[3]J.A. Dever, K.K. de Groh, B.A. Banks, J.A. Townsend, J.L. Barth, S. Thomson, T. Gregory, and W. Savage, *High Performance Polymers*, **12,** 125-139 (2000).

[4]Rockwell International Corporation 1990, Rocketdyne Division, Specification RC 1800 Review C, p. 18.
[5]Personal communication with Joshua Abel, Hubble Space Telescope CHAMP Program Lead Thermal Engineer, Lockheed Martin and Elisabeth Abel, Thermal Engineer, Lockheed Martin.
[6]American Society for Testing and Materials ASTM D 638-95, "Standard Test Method for Tensile Properties of Plastics," 1995.
[7]ASTM E 903-82, "Standard Test Method for Solar Absorptance, Reflectance, and Transmittance of Materials Using Integrating Spheres," American Society for Testing and Materials, 1982, Re-approved 1992.
[8]John H. Henninger, "Solar Absorptance and Thermal Emittance of Some Common Spacecraft Thermal Control Coatings," NASA RP 1121, 1984.
[9]J.A. Townsend, P.A. Hansen, J.A. Dever, K.K. de Groh, B.A. Banks, L. Wang, and C. He, *High Performance Polymers,* **11,** 81-99 (1999).
[10]K.K. de Groh, J.R. Gaier, R.L. Hall, M.P. Espe, D.R. Cato, J.K. Sutter, and D.A. Scheiman, 2000 *High Performance Polymers,* **12,** 83-104 (2000).
[11]K.K. de Groh and M. Martin, Journal of Spacecraft & Rockets, Vol. 41, No. 3, 366-372 (2004).
[12]R.P. Reed, R.E. Schramm, and A.F. Clark, *Cryogenics* **13,** 67–82 (1973).

REPORT DOCUMENTATION PAGE

Form Approved
OMB No. 0704-0188

1. AGENCY USE ONLY (*Leave blank*)	2. REPORT DATE	3. REPORT TYPE AND DATES COVERED
	October 2006	Technical Memorandum

4. TITLE AND SUBTITLE

Solar Effects on Tensile and Optical Properties of Hubble Space Telescope Silver-Teflon® Insulation

5. FUNDING NUMBERS

WBS–22R–251–30–0323–02

6. AUTHOR(S)

Kim K. de Groh, Joyce A. Dever, Aaron Snyder, Sharon Kaminski, Catherine E. McCarthy, Allison L. Rapoport, and Rochelle N. Rucker

7. PERFORMING ORGANIZATION NAME(S) AND ADDRESS(ES)

National Aeronautics and Space Administration
John H. Glenn Research Center at Lewis Field
Cleveland, Ohio 44135–3191

8. PERFORMING ORGANIZATION REPORT NUMBER

E–15572

9. SPONSORING/MONITORING AGENCY NAME(S) AND ADDRESS(ES)

National Aeronautics and Space Administration
Washington, DC 20546–0001

10. SPONSORING/MONITORING AGENCY REPORT NUMBER

NASA TM—2006-214336

11. SUPPLEMENTARY NOTES

Prepared for the 2006 Spring Meeting sponsored by the Materials Research Society, San Francisco, California, April 17–21, 2006. Kim K. de Groh, Joyce A. Dever, and Aaron Snyder, NASA Glenn Research Center; Sharon Kaminski, Catherine E. McCarthy, Allison L. Rapoport, and Rochelle N. Rucker, Hathaway Brown School, Shaker Heights, Ohio 44122. Responsible person, Kim K. de Groh, organization code RP, 216–433–2297.

12a. DISTRIBUTION/AVAILABILITY STATEMENT

Unclassified - Unlimited
Subject Categories: 18 and 27

Available electronically at http://gltrs.grc.nasa.gov

This publication is available from the NASA Center for AeroSpace Information, 301–621–0390.

12b. DISTRIBUTION CODE

13. ABSTRACT ***(Maximum 200 words)***

A section of the retrieved Hubble Space Telescope (HST) solar array drive arm (SADA) multilayer insulation (MLI), which experienced 8.25 yr of space exposure, was analyzed for environmental durability of the top layer of silver-Teflon (DuPont) fluorinated ethylene propylene (Ag-FEP). Because the SADA MLI had solar and anti-solar facing surfaces and was exposed to the space environment for a long duration, it provided a unique opportunity to study solar effects on the environmental degradation of Ag-FEP, a commonly used spacecraft thermal control material. Data obtained included tensile properties, solar absorptance, surface morphology and chemistry. The solar facing surface was found to be extremely embrittled and contained numerous through-thickness cracks. Tensile testing indicated that the solar facing surface lost 60 percent of its mechanical strength and 90 percent of its elasticity while the anti-solar facing surface had ductility similar to pristine FEP. The solar absorptance of both the solar facing surface (0.155±0.032) and the anti-solar facing surface (0.208±0.012) were found to be greater than pristine Ag-FEP (0.074). Solar facing and anti-solar facing surfaces were microscopically textured, and locations of isolated contamination were present on the anti-solar surface resulting in increased localized texturing. Yet, the overall texture was significantly more pronounced on the solar facing surface indicating a synergistic effect of combined solar exposure and increased heating with atomic oxygen erosion. The results indicate a very strong dependence of degradation, particularly embrittlement, upon solar exposure with orbital thermal cycling having a significant effect.

14. SUBJECT TERMS

Hubble Space Telescope; Environmental degradation, Extraterrestrial radiation; Teflon (DuPont); Thermal control insulation; Absorptance; Tensile properties

15. NUMBER OF PAGES

20

16. PRICE CODE

17. SECURITY CLASSIFICATION OF REPORT	18. SECURITY CLASSIFICATION OF THIS PAGE	19. SECURITY CLASSIFICATION OF ABSTRACT	20. LIMITATION OF ABSTRACT
Unclassified	Unclassified	Unclassified	